

# Photoionization model for streamer propagation mode change in simulation model for streamers in dielectric liquids

I Madshaven<sup>1</sup>, OL Hestad<sup>2</sup>,  
M Unge<sup>3</sup>, O Hjortstam<sup>3</sup>, PO Åstrand<sup>1</sup>‡

<sup>1</sup> Department of Chemistry, NTNU – Norwegian University of Science and Technology, 7491 Trondheim, Norway

<sup>2</sup> SINTEF Energy Research, 7465 Trondheim, Norway

<sup>3</sup> ABB Corporate Research, 72178 Västerås, Sweden

**Abstract.** Radiation is important for the propagation of streamers in dielectric liquids. Photoionization is a possibility, but the effect is difficult to differentiate from other contributions. In this work, we model radiation from the streamer head, causing photoionization when absorbed in the liquid. We find that photoionization is local in space ( $\mu\text{m}$ -scale). The radiation absorption cross section is modeled considering that the ionization potential (IP) is dependent on the electric field. The result is a steep increase in the ionization rate when the electric field reduces the IP below the energy of the first electronically excited state, which is interpreted as a possible mechanism for changing from slow to fast streamers. By combining a simulation model for slow streamers based on the avalanche mechanism with a change to fast mode based on a photoionization threshold for the electric field, we demonstrate how the conductivity of the streamer channel can be important for switching between slow and fast streamer propagation modes.

*Keywords:* Streamer, Prebreakdown, Dielectric Liquid, Photoionization, Simulation Model,

*Date:* 31 May 2022

‡ Corresponding author: [per-olof.aastrand@ntnu.no](mailto:per-olof.aastrand@ntnu.no)

## 1. Introduction

Dielectric liquids are widely used in high-voltage equipment, such as power transformers, because of their high electrical withstand strength and ability to act as a coolant [1]. If the electrical withstand strength of the liquid is exceeded, partial discharges followed by propagating discharges can occur and create prebreakdown channels called “streamers”. Streamers are commonly classified by their polarity and propagation speed, ranging from below 0.1 km/s for the 1st mode to above 100 km/s for the 4th mode [2]. Streamers can be photographed by schlieren techniques, which captures the difference in permittivity between the gaseous streamer channel and the surrounding liquid [3], or by capturing light emitted by the streamer [4]. Continuous dim light has been observed from both the streamer channel and the streamer tip [5], as well as bright light from the streamer tip and re-illuminations of the streamer channel [5, 6]. The intensity of the emitted light and the occurrence of re-illuminations increases with higher streamer propagation modes. Photoionization by light absorbed in the liquid has been proposed as a possible feed-forward mechanism involved in the fast 3rd and 4th mode streamers [6, 7].

Streamer propagation is a multiscale, multiphysics phenomenon involving numerous mechanisms and processes [2]. Developing predictive models and simulations is challenging, but many attempts exist [8, 9]. Simulations have often focused on one aspect of the problem, such as the electric field [10, 11], production of free electrons [12], conductance of the streamer channels [13], inhomogeneities [14], or the plasma within the channels [15].

In this work we investigate a model for photoionization [16, 17] and combine it with a simulation model for propagation of streamers through an avalanche mechanism [18, 19]. Theory on molecular energy states and radiation is given in the next section. The photoionization model is presented, evaluated and discussed in sections 3, 4 and 5, respectively. Section 6 describes the simulation model based on electron avalanches, with photoionization included, and the results of this model is presented section 7. The model and the results are discussed in section 8, with the main conclusions summarized in section 9.

## 2. Molecular energy states and radiation

Molecules exist in quantum states with different energy  $\mathcal{E}_n$ . Excitation to a state of higher energy or relaxation to a state of lower energy can be achieved by absorbing or emitting a photon, respectively. The energy difference between molecular vibrational states is in the range meV to about 0.5 eV, while molecular electronic

states have energies from some eV and up to around 20 eV. Change in vibrational states corresponds to infrared (IR) radiation (room temperature is about 25 meV), whereas visible (VIS) light (1.7–3.1 eV) and ultraviolet (UV) light (above 3.1 eV) normally correspond to electronic excitations. The transition probabilities to lower states gives the lifetime of an excited state, which varies from fs to several  $\mu$ s. In the case of fluorescence, an excited molecule relaxes through one or more states, before relaxing to the electronic ground state. The final relaxation is the most energetic and has the longest decay time, e.g. about 7.3 eV and 1 ns in liquid cyclohexane [20].

The ionization potential (IP) of a molecule is the energy required to excite an electron from the ground state  $\mathcal{E}_0$  to an unbound state. Applying an external electric field  $\mathbf{E}$  decreases the IP [21]

$$\mathcal{E}_{\text{FDIP}}(E, \theta_e) = \mathcal{E}_{\text{IP}} - \beta \cos \theta_e \sqrt{\frac{E}{\epsilon_r E_{a_0}}}, \quad (1)$$

where  $\mathcal{E}_{\text{IP}}$  is the zero-field IP,  $E_{a_0} = 5.14 \times 10^{11}$  V/m,  $\epsilon_r$  is the relative permittivity of the liquid,  $\cos \theta_e = \hat{\mathbf{k}}_e \cdot \hat{\mathbf{E}}$ , and  $\mathbf{k}_e$  is the momentum of emitted electron. The parameter  $\beta = 54.4$  eV for the hydrogen atom, and has been estimated from calculations on atoms and molecules [21]. The energy of excited states is usually not significantly affected by the electric field in comparison to the field-dependence of the IP [21–23].

Spectral analysis of the light emitted from streamers show a broad band of photon energies up towards 3–4 eV [31, 32]. Distinct peaks in the emission spectrum reveal the presence of entities such as  $\text{H}_2$ ,  $\text{C}_2$ , and  $\text{CH}_4$ , which are likely products of dissociation and recombination of hydrocarbon molecules from the base liquid [31, 33]. Stark broadening of the  $\text{H}_\alpha$ -line can be investigated to find electron densities above  $10^{24} \text{ m}^{-3}$ , while the relation between the  $\text{H}_\alpha$  and the  $\text{H}_\beta$ -line point to electron temperatures in the area of 10 kK [34]. Furthermore, rotational and vibrational temperatures of several kK can be estimated from spectral emission of  $\text{C}_2$  Swan bands [35].

During a streamer breakdown, electrons (and other charged particles) are gaining energy and are accelerated in the electric field. Energy can be exchanged with other particles through collisions, possibly resulting in excitation, ionization or dissociation of molecules. Subsequently, relaxation or recombination can cause photon emission. The radiation  $B$  is absorbed by the medium, given by  $\nabla B = -B\sigma\rho$ , where  $\sigma$  is the absorption cross section and  $\rho$  is the number density of the medium. In spherical symmetry,

$$B(r) = B_0 \left(\frac{r_0}{r}\right)^2 \exp\left(-\int_{r_0}^r \rho \sigma \, d\ell\right), \quad (2)$$

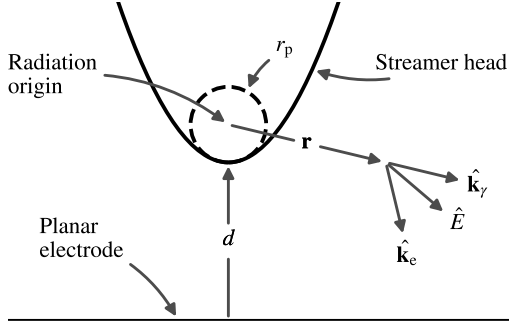


**Figure 1.** Sketch of a hyperbolic streamer head and relevant variables.

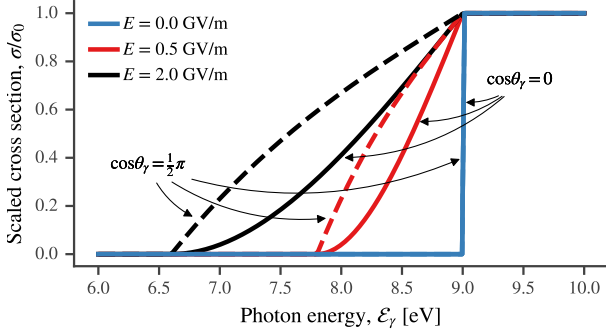


**Figure 2.** Photoionization cross section  $\sigma$  for different electric fields  $E$  and angles  $\theta_\gamma$  as a function of photon energy  $\mathcal{E}_\gamma$ , calculated from (5) combined with (1).

where  $\mathbf{B}(r = r_0) = \mathbf{B}_0 = B_0 \hat{\mathbf{r}}$ . The ionization cross section of cyclohexane, for instance, increases from close to zero below the IP to about  $5 \times 10^{-21} \text{ m}^2$  over the range of around 1 eV [36]. For single photons, cyclohexane begins to absorb around the first excitation energy and the absorption cross section increases steadily for higher photon energies [37]. A streamer could generate high-energy photons, which are rapidly absorbed by the liquid and therefore not measured by experiments [31].

The photon number density  $n_\gamma$  is related to the radiance  $B$ ,  $n_\gamma = B/\mathcal{E}_\gamma c$  [38], where  $\mathcal{E}_\gamma$  is the photon energy and  $c$  is the speed of light in vacuum. It follows that the change in photon density is  $\nabla n_\gamma = -n_\gamma \sigma \rho$  and that the ionization rate is  $W = n_\gamma \sigma \rho c$ . However, generally  $B = B(\mathcal{E}_\gamma)$  and integration is needed to calculate  $W$  and the ionization rate per molecule  $w$ ,

$$w(r) = \frac{W}{\rho} = \int \frac{B(r, \mathcal{E}_\gamma) \sigma(r, \mathcal{E}_\gamma)}{\mathcal{E}_\gamma} d\mathcal{E}_\gamma. \quad (3)$$

For instance,  $w = 10^{-2} / \mu\text{s}$  implies that 1 % of the molecules would be ionized within a  $\mu\text{s}$ .

### 3. Defining the streamer radiation model

Streamers can emit light sporadically from the channel (re-illuminations) and continuously from the streamer

head, with fast streamers emitting more light than slow streamers [6]. In this work, we investigate the possibility of light emitted from the gaseous streamer head causing ionization in the liquid, resulting in a change to a faster streamer mode.

The probability of emitting the electron in a given direction is dependent on the momentum of the absorbed photon, i.e. the differential cross section  $d\sigma$  is dependent on the differential solid angle  $d\Omega$ ,

$$d\sigma \propto \sin^2 \theta d\Omega, \quad (4)$$

where  $\cos \theta = \hat{\mathbf{k}}_e \cdot \hat{\mathbf{k}}_\gamma$ . When  $\mathcal{E}_\gamma < \mathcal{E}_{\text{IP}}$  we solve for  $\mathcal{E}_\gamma = \mathcal{E}_{\text{FDIP}}(E, \Theta)$  in (1) to find the maximum possible angle  $\Theta$  of electron emission. Then integrate (4) over all angles where  $\theta < \Theta$  to arrive at an expression for the photoionization cross section

$$\begin{aligned} \sigma/\sigma_0 = 1 - \frac{1}{4}(1 + \cos^2 \theta_\gamma)(3 \cos \Theta - \cos^3 \Theta) \\ - \frac{1}{2} \sin^2 \theta_\gamma \cos^3 \Theta, \end{aligned} \quad (5)$$

where  $\cos \theta_\gamma = \hat{\mathbf{k}}_\gamma \cdot \hat{\mathbf{E}}$ . Equation (5) has been scaled such that  $\sigma(\Theta = 0) = 0$  and  $\sigma(\Theta = \frac{1}{2}\pi) = \sigma_0$ . This is illustrated by figure 2, where  $\sigma = 0$  when  $\mathcal{E}_\gamma < \mathcal{E}_{\text{FDIP}}$ ,  $\sigma = \sigma_0$  when  $\mathcal{E}_\gamma > \mathcal{E}_{\text{IP}}$ , and dependent on  $E$  and  $\mathbf{k}_\gamma$  when  $\mathcal{E}_{\text{FDIP}} < \mathcal{E}_\gamma < \mathcal{E}_{\text{IP}}$ .

We choose  $z = (d + r_p)$  as the origin of radiation with a radiance  $\mathbf{B}(r = r_p) = \mathbf{B}_0$ , see figure 1. Generally,  $B_0$  is comprised of a distribution of photon energies, however, we choose to limit the model to only consider radiation from a single low-energy excited state ( $\mathcal{E}_\gamma = \mathcal{E}_n - \mathcal{E}_0$ ), since low-energy states are likely the most abundant ones. Radiation can cause ionization if the photon energy exceeds the field-dependent IP, i.e.  $\mathcal{E}_\gamma > \mathcal{E}_{\text{FDIP}}$ . Prolate spheroid coordinates are used to calculate the Laplacian electric field magnitude and direction [18], in order to calculate  $\sigma$  by (5). The radiance  $\mathbf{B}$  in (2) and the ionization rate  $w$  in (3) can then be calculated, assuming low density ( $\rho \approx 0$ ) within the streamer head and constant density in the liquid. The integration of  $\sigma$  is performed numerically in a straight line from  $z = (d + r_p)$ . Two-photon excitations (absorption to excited states) and scattering (absorption and re-emission) are assumed to have low influence and are ignored in this work.

### 4. Properties of the radiation model

To evaluate the radiation model, a hyperbolic streamer head with tip curvature  $r_p = 6 \mu\text{m}$  is placed with a gap  $d = 10 \text{ mm}$  towards a planar electrode (see figure 1). The model liquid is similar to cyclohexane, assuming radiation from the lowest excited state, i.e.  $\mathcal{E}_\gamma = \mathcal{E}_1 - \mathcal{E}_0 = 7 \text{ eV}$ ,  $\mathcal{E}_{\text{IP}} = 9 \text{ eV}$ ,  $\sigma_0 = 10^{-21} \text{ m}^2$  and  $\rho = 5.6 \times 10^{27} / \text{m}^3$  [16]. The initial power of the radiation is set to  $B_0 = 1 \text{ W}/\mu\text{m}^2$ , which is in the range

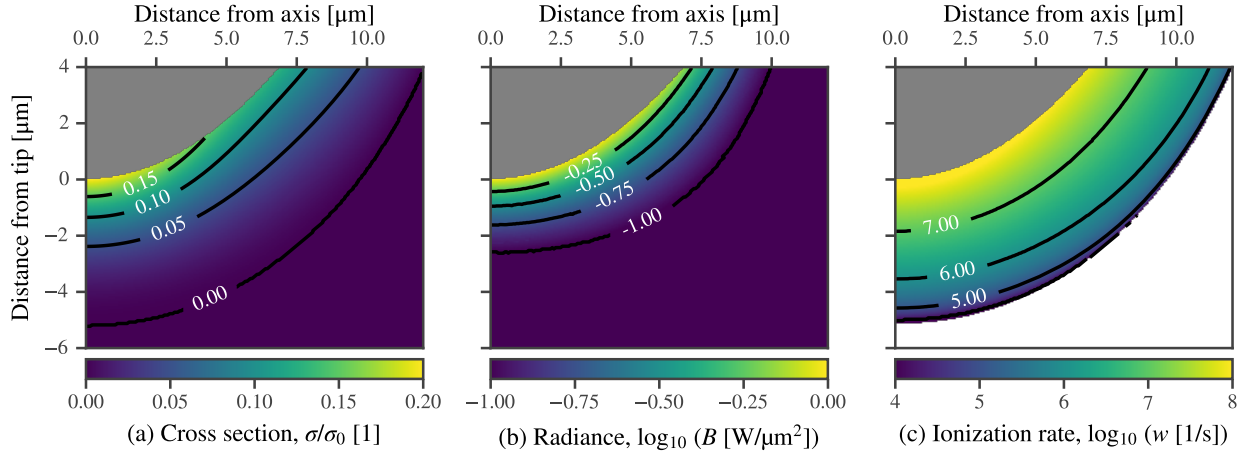


**Figure 3.** Streamer head (in grey) with  $r_D = 6 \mu\text{m}$  and  $V_0 = 100 \text{ kV}$ , placed  $d = 10 \text{ mm}$  from the planar electrode. The cross section (a), radiance (b), and photoionization rate (c) are calculated by (5), (2), and (3), respectively, applying the parameter values stated in the first paragraph of section 4. The  $y$ -axis is equal for all the plots.

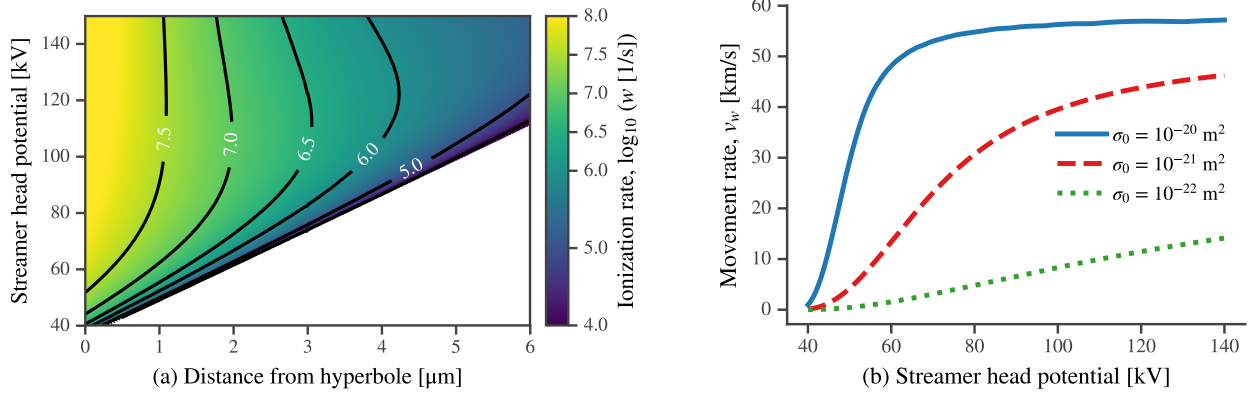


**Figure 4.** (a) Ionization rate  $w$  along  $z$ -axis for different  $V_0$ .  $100 \text{ kV}$  corresponds to figure 3(c). (b) Maximum movement rate  $v_w$  calculated by (6) assuming  $p = 0.001$ . The transition is sharpest for  $\sigma_0 = 10^{-20} \text{ m}^2$  followed by  $10^{-21} \text{ m}^2$ , while  $10^{-22} \text{ m}^2$  resembles a linear increase. The magnitude is linearly dependent on  $B_0$  and inversely dependent on  $p$ .

of the power needed to evaporate the liquid [39]. The actual radiation power of a streamer is unknown and likely to fluctuate. However, since the results are linear in  $B_0$ , setting a value enables a discussion of whether the results are reasonable.

The area where ionization is possible increases with  $V_0$  and covers a range of about  $5 \mu\text{m}$  from the streamer head when  $V_0 = 100 \text{ kV}$ , see figure 3(a). At the  $z$ -axis,  $\sin \theta_\gamma = 0$ , the cross section  $\sigma$  is yet the largest close to the streamer head, because of the strong electric field  $E$ . Figure 3(a) shows how  $\sigma$  declines as the distance from the streamer head increases. One could expect that  $\sigma$  would decline fast close to the streamer head as the distance from the  $z$ -axis increases, since  $E$  declines, however, an increase in  $\sin \theta_\gamma$  when moving away off-axis counteracts the reduction in  $E$ , resulting in just a slight decrease in  $\sigma$ . Numeric integration of  $\sigma$  in figure 3(a) is applied to find  $B$  in (2), see figure 3(b). The rapid decay of the radiance is expected considering that  $\rho\sigma_0 = 5.6/\mu\text{m}$  (i.e. a penetration

depth of  $\delta = 1/\sigma\rho = 0.18 \mu\text{m}$ ) is included in the exponent in (2). The ionization rate per molecule  $w$  in (3) is presented in figure 3(c). A major finding is that photoionization is indeed a very local effect in dielectric liquids, mainly occurring within a few  $\mu\text{m}$  of the source, which is the streamer head in this case.

Increasing  $V_0$  increases the ionization rate  $w$  close to the streamer head and increases the reach of the ionization zone in figure 4(a). We may hypothesize that photoionization cause streamer propagation once a degree of ionization  $p$  is obtained. The time required to reach  $p$  is inversely dependent on the ionization rate  $w$ , which varies with the distance from the streamer head  $\Delta r$ . From this we define the photoionization speed of the streamer,

$$v_w = \max \left\{ \frac{\Delta r w}{p} \right\}. \quad (6)$$

The values for  $\Delta r$  and  $w$  is calculated numerically for a range close to the streamer head and  $v_w$  is set to

the maximum value of their product. Since measured electron densities in streamers point to a degree of ionization in the range of 0.1 % to 1 %. [34, 35], we assume that  $p = 0.001$  is required for propagation. The photoionization speed  $v_w$  of the data in figure 4(a) is presented in figure 4(b), showing an increase in  $v_w$  as  $\mathcal{E}_{\text{FDIP}}$  is reduced below  $\mathcal{E}_\gamma$ . Physically, when the liquid no longer can absorb light to a bound excited state, the result is direct ionization, and it is reasonable that ionization contributes more to the propagation speed than emission of light or local heating. The transition from low to high speed (low to high ionization rate) in figure 4(b) for the largest cross section ( $\sigma_0 = 10^{-20} \text{ m}^2$ ) occurs over a short voltage range of about 20 kV.

## 5. Discussion of the radiation model

The modeled photoionization cross section increased from zero towards a maximum of  $10^{-21} \text{ m}^2$ , which resulted in rapid absorption within a few  $\mu\text{m}$ . The real absorption might be even more rapid, since the cross section of cyclohexane is about 5 times larger for ionizing radiation [36]. Increasing the cross section  $\sigma$  gives a shorter penetration depth  $\delta = 1/\sigma\rho$ , and results in a shorter range for the radiance and ionization in figure 3, giving a sharper transition in the movement rate  $v_w$  in figure 4(b). The fluorescence of cyclohexane is consistent with radiation from the first excited state [20], but the absorption to this state is intrinsically low [37]. Radiation from fluorescence may thus transport energy away from the streamer head.

Excited molecules in the liquid have a high probability of non-radiative relaxation which heats the liquid. In strong electric fields, the IP is reduced and bound excited states become unbound, i.e. they appear above the ionization threshold [22], and instead of heating, absorption causes ionization. It is, however, difficult to assess how an electric field affects cross sections. By assuming an increase in the cross section when the field is increased (see figure 2), more radiation is absorbed, but the effect also becomes more local. The model therefore predicts a faster propagation when the radiation from the streamer head is absorbed directly in front of the streamer, in line with figure 4(b) where higher cross sections results in higher speeds.

The photoionization cross sections  $\sigma$  for linear alkanes and aromatics differ by more than a decade, from about  $1 \times 10^{-22} \text{ m}^2$  to  $5 \times 10^{-21} \text{ m}^2$  [40]. Given a number density  $\rho = 5 \times 10^{27} / \text{m}^3$ , the penetration depth  $\delta$  is between  $2 \mu\text{m}$  and  $0.04 \mu\text{m}$ , respectively. Ionizing radiation emitted when electrons recombine with cations is therefore rapidly absorbed, however, non-ionizing radiation having lower absorption cross section can propagate further. If we assume that fluorescent radiation from cyclohexane is absorbed with a cross

section of  $1/100$  of the ionizing radiation, this radiation has a reach of several  $\mu\text{m}$ . In combination with a low-IP aromatic additive, having a larger cross section, the reach of the radiation is reduced, but radiation absorbed by the additive causes ionization whereas absorption to cyclohexane resulted in heat. Low-IP additives are suggested to increase the acceleration voltage by increasing the number of branches of a streamer [24]. Increased branching can stabilize the streamer through electrostatic shielding, however, photoionization in front of the streamer can be involved in a change to a fast mode [6, 7]. For instance, pyrene ( $\mathcal{E}_{\text{IP}} = 7 \text{ eV}$  [23]) is ionized when absorbing fluorescent radiation from cyclohexane, and could facilitate streamer growth by providing seed electrons for new avalanches. A similar result is found for gases where additives absorbing ionizing radiation can increase the streamer propagation speed for a single branch [41].

Studies in natural ester found that having an additive absorbing UV with energy comparable to the first excited state of the ester increases the acceleration voltage [26, 27]. Rather than regulation through branching, it is suggested that absorbing UV close to the streamer prevents the generation of seed electrons farther away from the streamer head [27]. As such, the available excited states and absorption probabilities are important to consider. Pyrene has excited states between 3 eV and 6 eV [23] and can thus absorb and radiate energy which is generally not absorbed by cyclohexane. Pyrene and dimethylaniline (DMA) have a similar  $\mathcal{E}_{\text{IP}}$  and first excitation energy, and both additives increase the acceleration voltage in cyclohexane [24, 28]. However, whereas pyrene absorbs radiation at the lowest excitation energy which is a  $\pi$  to  $\pi^*$  transition, the lowest excited state of DMA is non-absorbing [29] and thus the second lowest excitation energy should be considered instead. It is not uncommon that the lowest state is non-absorbing. For example in azobenzenes, also studied as an additive in streamer experiments, the lowest  $n$  to  $\pi^*$  transition is non-absorbing, whereas the second excitation,  $\pi$  to  $\pi^*$ , has a high absorbance and gives the molecules their color [30]. Furthermore, the first excited state in cyclohexane has a lifetime of about a ns [20], which gives some possibility for a two-photon ionization, however, excited states of the additives can have lifetimes of tens to hundreds of ns [42], making two-photon ionization more probable.

There is a relatively small number of electronic states available below the IP, but a large number of states above the IP, often considered as a continuum. This makes the cross section for ionization larger than the cross section for absorption to a bound excited state. Consequently, as the IP decreases with an increase in the electric field, the cross section at certain energies

increases. A local electric field in excess of 0.5 GV/m is sufficient to remove all excited states of cyclohexane in gas phase [22]. In a liquid where  $\epsilon_r = 2$ , we find that a local field of 1.4 GV/m reduce the IP by 2 eV from (1), which is sufficient to reduce  $\mathcal{E}_{\text{FDIP}}$  below the first excited state in cyclohexane. When the electric field is above this threshold, cyclohexane cannot absorb radiation to a bound state and is ionized instead. For a hyperbolic streamer head with  $r_p = 6 \mu\text{m}$  in a gap  $d = 10 \text{mm}$ , this threshold is reached at a potential of 37 kV, assuming that the local field is the same as the macroscopic field, and the transition in speed occurs above this in figure 4(b). The threshold is close to the acceleration voltage in a tube [43], but much lower than the acceleration voltage in a non-constricted large gap [24]. However, the actual tip radius of the streamer and the degree of branching are important when calculating the tip field, as well as space charge generated in the liquid. Furthermore, the local field can differ from the macroscopic field. For instance, the field is increased by a factor of 1.3 in a spherical cavity in a non-polar liquid [21]. The model mainly demonstrates how rapid ionizing radiation (high cross section) is absorbed in the liquid.

## 6. Avalanche model with photoionization

In earlier work we have developed a model for simulating the propagation of positive streamers in non-polar liquids through an electron avalanche mechanism [18, 19]. Here we incorporate the photoionization mechanism into the streamer model. A short overview of the model is given below.

Simulation parameters are similar with those used in our previous works, i.e. a needle-plane gap with cyclohexane as a model liquid. The needle is represented by a hyperbole (see figure 1) with tip curvature  $r_n = 6.0 \mu\text{m}$ , placed  $d = 10 \text{mm}$  above a grounded plane. The potential  $V_0$  applied to the needle gives rise to an electric field  $\mathbf{E}$  in the gap. The Laplacian electric field is calculated analytically in prolate spheroid coordinates. Electrons detach from anions in the liquid (assumed ion density  $n_{\text{ion}} = 2 \times 10^{12} \text{m}^{-3}$ ) and grow into electron avalanches if the field is sufficiently strong. The number of electrons  $N_e$  in an avalanche is given by

$$\ln N_e = \sum_i E_i \mu_e \alpha_m e^{-E_\alpha/E_i} \Delta t, \quad (7)$$

where  $\alpha_m = 130/\mu\text{m}$  and  $E_\alpha = 1.9 \text{GV/m}$  for cyclohexane [44],  $\mu_e = 45 \text{mm}^2/\text{Vs}$  is the electron mobility,  $i$  denotes a simulation iteration, and  $\Delta t = 1 \text{ps}$  is the time step. If an avalanche obtains a number of electrons  $N_e > 10^{10}$ , it is considered ‘‘critical’’. The streamer grows by placing a new streamer head wherever an avalanche becomes critical. Each streamer

head, an extremity of the streamer, is represented by a hyperbole with tip curvature  $r_s = 6.0 \mu\text{m}$ . After the inception of the streamer, the electric potential  $V$  and the electric field  $\mathbf{E}$  for a given position  $\mathbf{r}$  is calculated by a superposition of the needle and all the streamer heads,

$$V(\mathbf{r}) = \sum_i k_i V_i(\mathbf{r}), \quad \mathbf{E}(\mathbf{r}) = \sum_i k_i \mathbf{E}_i(\mathbf{r}), \quad (8)$$

where  $i$  denotes a streamer head. The coefficients  $k_i$  correct for electrostatic shielding between the heads. Whenever a new head is added, the streamer structure is optimized, possibly removing one or more existing heads. Streamer heads within  $50 \mu\text{m}$  of another head closer to the plane, and heads with  $k_i < 0.1$ , are removed [18].

Each streamer head is associated with a resistance in the channel towards the needle and a capacitance in the gap towards the planar electrode [19]. The resistance  $R$  and capacitance  $C$  is given by

$$R \propto \ell, \quad \text{and} \quad C \propto \left( \ln \frac{4z + 2r_s}{r_s} \right)^{-1}, \quad (9)$$

where  $\ell$  is the distance from the needle to the streamer head and  $z$  is the position of the streamer head in the gap. New streamer heads are given a potential which magnitude depends on their position as well as the configuration of the streamer. The potential  $V_i$  of each streamer head is relaxed towards the potential of the needle electrode  $V_0$  each simulation time step. This is achieved by reducing the difference in potential,

$$\Delta V_i = V_0 - V_i \rightarrow V_i = V_0 - \Delta V_i e^{-\Delta t/\tau_i}, \quad (10)$$

where the time constant is given by  $\tau = \tau_0 RC$  and  $\tau_0 = 1 \mu\text{s}$ . If the electric field within the streamer channel  $E_s = \Delta V_i/\ell_i$  exceeds a threshold  $E_{\text{bd}}$ , a breakdown in the channel occurs, equalizing the potential of the streamer head and the needle. A channel breakdown affects the potential of a single streamer head since each streamer head is ‘‘individually’’ connected to the needle [19].

Calculating the photoionization cross section in (5) is a computational expensive operation, contrary to our avalanche simulation model which is intended to be relatively simple and computationally efficient. The photoionization model indicates an increase in speed (see figure 4) when  $\mathcal{E}_{\text{FDIP}} < \mathcal{E}_n$  over a short distance into the liquid. To model photoionization in an efficient way, we add a ‘‘photoionization speed’’  $v_w$  to each streamer head exceeding a threshold  $E_w = 3.1 \text{GV/m}$ . This is implemented by moving such streamer heads a distance  $\mathbf{s}_w = v_w \Delta t \hat{\mathbf{z}}$ . Equation (6) predicts a speed  $v_w$  given a set of parameter values (see figure 4(b)), where some, such as radiation power and degree of ionization, are unknown. The chosen power of  $1 \text{W}/\mu\text{m}^2$  exceeds

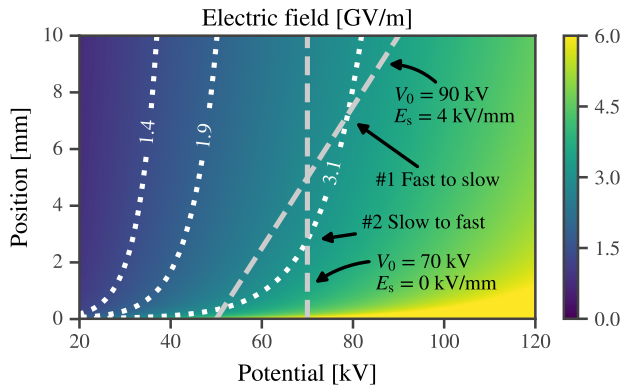


**Figure 5.** Electric field strength at the tip of an electric hyperboloid with a tip curvature of  $6.0 \mu\text{m}$  for a given position and potential. The dotted white lines show the electric field thresholds for IP reduction by  $2 \text{ eV}$  ( $1.4 \text{ GV/m}$ ) and  $3 \text{ eV}$  ( $E_w = 3.1 \text{ GV/m}$ ), as well as  $E_\alpha = 1.9 \text{ GV/m}$ . The dashed gray lines represent streamers. (1) indicate how an electric field of  $E_s = 4 \text{ kV/mm}$  can change the propagation mode from fast to slow in the beginning of the gap. (2) indicate how a highly conducting streamer can change from slow to fast towards the end of the gap.

$100 \text{ W}$  in total when distributed over a streamer head with a radius of some  $\mu\text{m}$ . Since a streamer requires about  $5 \text{ mJ/m}$  for propagation [39], the expected speed exceeds  $20 \text{ km/s}$ , which is in line with figure 4(b). We choose  $v_w = 20 \text{ km/s}$  for the simulations, which is the order of magnitude given by figure 4(b), but slow compared to some 4th mode streamers exceeding  $100 \text{ km/s}$ . However, this is sufficient to investigate transitions between slow and fast mode since it is more than an order of magnitude above the speed predicted by the simulations without a photoionization contribution [18].

## 7. Results from avalanche model with photoionization

For evaluating the model we investigate the influence of the applied voltage  $V_0$  (square wave), the threshold for breakdown in the channel  $E_{bd}$ , while excluding or including photoionization. Figure 5 illustrates the behavior of two different single head streamers. Streamer 1 starts in a fast mode, but after propagating some mm the electric field at the streamer head has dropped below the threshold for fast propagation  $E_w$  and the streamer changes to a slower mode of propagation. Streamer 2 starts in a slow mode, but having no potential drop within the streamer channel, the electric field at the streamer head increases during propagation and the streamer changes to a fast mode for the final few mm of the gap.

Both streamer 1 and 2 in figure 5 are simplified cases with a single head and a constant  $E_s$ , however, the simulations in figure 6(a) show a similar behavior, but at higher voltages. In the simulations with low

$E_{bd}$ , resulting in a low  $E_s$ , the streamers switch to fast mode for the final portion of the gap, and the portion increases with increasing voltage. According to figure 5, all of the streamers in figure 6(a) starts above the threshold of  $E_w = 3.1 \text{ GV/m}$ , however, as the streamer propagates and more streamer heads are added, electrostatic shielding between the heads quickly reduces the electric field below this threshold. Increasing  $E_{bd}$  gives an on average higher  $E_s$  and figure 6(a) illustrates how this can make streamers change between fast and slow propagation. Figure 6(b) details a streamer beginning in fast mode and changing to slow propagation mode. Propagation reduces the potential at the streamer head. When the electric field at the tip is sufficiently reduced, the streamer changes to a slow mode. Re-illuminations, breakdowns within the streamer channel, sporadically increases the potential and can push the streamer over in a fast mode, however, often this “fast mode” is brief and difficult to notice.

By considering a wider range of voltages in figure 7, the transition from slow to fast mode occurs at about  $100 \text{ kV}$  for a highly conducting streamer. Increasing  $E_{bd}$  decreases the average (in time) electric field at the streamer heads and thus delays the onset of the fast mode to about  $120 \text{ kV}$ . As mentioned in our previous work, the propagation voltage predicted by the simulations is somewhat high compared with experiments, whereas the propagation speed is low for second mode streamers [18]. The present work does not aim to improve on these limitations for slow streamers, but rather demonstrate how changes between slow and fast propagation can occur in different parts of the gap. The propagation speed for slow-mode streamers is about ten times of that predicted by figure 7, but the difference can be removed by assuming a higher electron mobility or a higher seed density [18].

## 8. Discussion

The role of photoionization during discharge in liquids is difficult to assess. For breakdown in gases, ionizing radiation can penetrate far into the medium, providing seed electrons for avalanches. While similar reasoning have been suggested for liquids, we argue that, given the higher density of the liquid and the large cross section for ionizing radiation, the penetration depth is short and photoionization occurs locally. Low-energy radiation have longer range and can provide seed electrons through a two-step ionization process. However, ionization of impurities or additives are far more likely, especially when the radiation from the base liquid can ionize them directly or they have long-lived excited states.

Assuming that increasing the applied potential increases the amount of radiation, it also increases

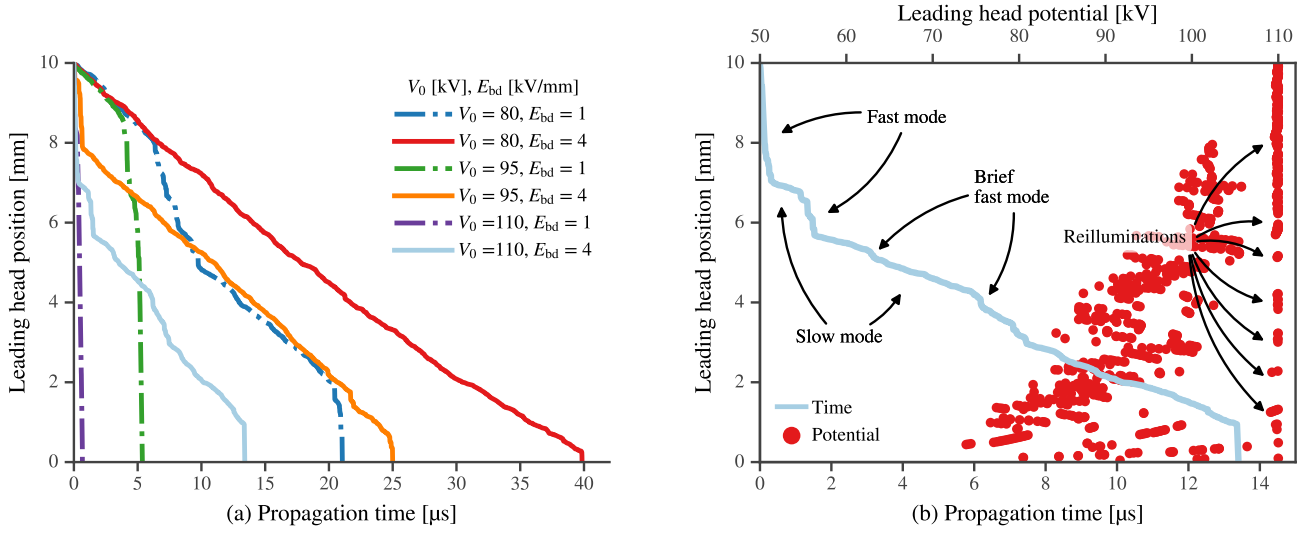


**Figure 6.** (a) Streak plots showing the position of the leading streamer head as a function of time. The transition from slow to fast or from fast to slow is dependent on the needle potential and the channel breakdown threshold. (b) Propagation time and leading head potential as a function of leading head position in the gap for  $V_0 = 110$  kV and  $E_{bd} = 4$  kV/mm in (a).

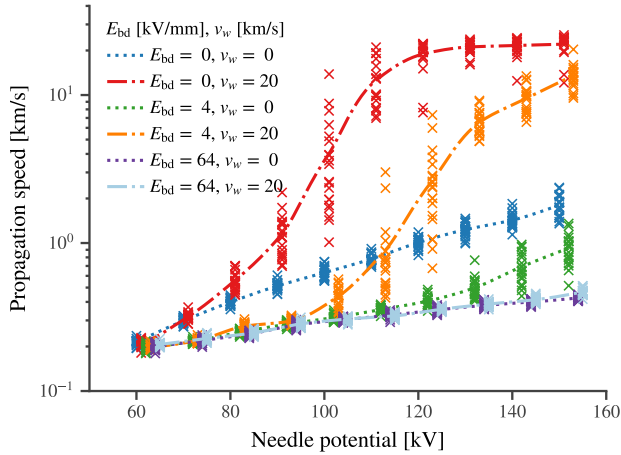


**Figure 7.** Average propagation speed for the middle of the gap ( $z$  between 2.5 mm and 7.5 mm). The onset of the fast mode is delayed when the field within the streamer channel is increased. Each marker is a simulation (20 for each voltage, 1200 in total) and the lines are interpolated to the average.  $v_w = 0$  km/s implies no added speed from photoionization.

generation of seed electrons for avalanches. Seeds likely facilitates both propagation speed and branching, while electrostatic shielding between branches can regulate the propagation speed. One hypothesis is that the change to a fast mode occurs when one fast branch escapes the electrostatic shielding from the others. If the radiation from such a branch can penetrate deep into the liquid, energy is transported away from the streamer head, while new seeds and subsequent avalanches can result in electrostatic shielding. Both of these mechanisms can reduce the speed. However, we have presented a model where a strong electric

field makes photoionization more localized, suppressing energy transport and branching. This can explain how a streamer changes to a fast propagation mode when the electric field is sufficiently strong.

The model is limited in the sense that we do not know the actual value for the radiated power (or its energy distribution) or the degree of ionization it takes for a streamer to propagate. To assess the model we chose a value for the radiated power, and showed that this would be sufficient to ionize the liquid at a reasonable rate. Whether obtaining this radiated power is feasible remains unknown.

## 9. Conclusion

Emission and absorption of light may be important for streamer propagation. Radiation can transport energy away from the streamer as heat or create free electrons through ionization, however, ionizing radiation is rapidly absorbed and thus unlikely to create seed electrons at some distance from the streamer head. Furthermore, since increasing the electric field reduces the ionization potential, it also increases the ionization cross section, making photoionization a local process. The model based on the electron avalanche mechanism in combination with modeling photoionization close to the streamer tip is found to capture the feature of acceleration of the streamer tip above a critical voltage. The photoionization model is missing a proper estimation of the spectral intensity of the radiation as well as the resulting speed, and this need to be investigated in the future. Radiation and photoionization is often mentioned in streamer literature, however, the potential short reach of the

ionizing radiation is an important aspect to consider in understanding streamers in dielectric liquids.

### Acknowledgment

This work has been supported by The Research Council of Norway (RCN), ABB and Statnett, under the RCN contract 228850.

### References

- [1] Wedin P (2014) *IEEE Electr Insul Mag* **30**:20–25
- [2] Lesaint O (2016) *J Phys D: Appl Phys* **49**:144001
- [3] Farazmand B (1961) *Br J Appl Phys* **12**:251–254
- [4] Sakamoto S, Yamada H (1980) *IEEE Trans Electr Insul* **EI-15**:171–181
- [5] Dung NV, Høidalen HK, Linhjell D, Lundgaard LE, Unge M (2013) *J Phys D: Appl Phys* **46**:255501
- [6] Linhjell D, Lundgaard L, Berg G (1994) *IEEE Trans Dielectr Electr Insul* **1**:447–458
- [7] Lundgaard L, Linhjell D, Berg G, Sigmond S (1998) *IEEE Trans Dielectr Electr Insul* **5**:388–395
- [8] Biller P (1996) In *ICDL'96 12th Int Conf Conduct Break Dielectr Liq*, 189–192. IEEE
- [9] Beroual A (2016) In *2016 IEEE Electr Insul Conf*, 117–128
- [10] Niemeyer L, Pietronero L, Wiesmann HJ (1984) *Phys Rev Lett* **52**:1033–1036
- [11] Fofana I, Beroual A (1998) *Jpn J Appl Phys* **37**:2540–2547
- [12] Kim M, Hebner R, Hallock G (2008) *IEEE Trans Dielectr Electr Insul* **15**:547–553
- [13] Kupershtokh AL, Karpov DI (2006) *Tech Phys Lett* **32**:406–409
- [14] Jadidian J, Zahn M, Lavesson N, Widlund O, Borg K (2014) *IEEE Trans Plasma Sci* **42**:1216–1223
- [15] Naidis GV (2016) *J Phys D: Appl Phys* **49**:235208
- [16] Madshaven I, Smalø HS, Unge M, Hestad OL (2016) In *2016 IEEE Conf Electr Insul Dielectr Phenom*, 400–403
- [17] Madshaven I, Åstrand PO, Hestad OL, Unge M, Hjortstam O (2017) In *2017 IEEE 19th Int Conf Dielectr Liq*, 1–4
- [18] Madshaven I, Åstrand PO, Hestad OL, Ingebrigtsen S, Unge M, Hjortstam O (2018) *J Phys Commun* **2**:105007
- [19] Madshaven I, Hestad OL, Unge M, Hjortstam O, Åstrand PO (2019) *Plasma Res Express* doi: 10/c933
- [20] Wickramaaratchi MA, Preses JM, Holroyd RA, Weston RE (1985) *J Chem Phys* **82**:4745–4752
- [21] Smalø HS, Hestad OL, Ingebrigtsen S, Åstrand PO (2011) *J Appl Phys* **109**:073306
- [22] Davari N, Åstrand PO, Ingebrigtsen S, Unge M (2013) *J Appl Phys* **113**:143707
- [23] Davari N, Åstrand PO, Unge M (2015) *Chem Phys* **447**:22–29
- [24] Lesaint O, Jung M (2000) *J Phys D: Appl Phys* **33**:1360–1368
- [25] Ingebrigtsen S, Smalø HS, Åstrand PO, Lundgaard LE (2009) *IEEE Trans Dielectr Electr Insul* **16**:1524–1535
- [26] Unge M, Singha S, Van Dung N, Linhjell D, Ingebrigtsen S, Lundgaard LE (2013) *Appl Phys Lett* **102**:172905
- [27] Liang S, Wang F, Huang Z, Chen W, Wang Y, Li J (2019) *IEEE Access* **7**:73448–73454
- [28] Linhjell D, Ingebrigtsen S, Lundgaard L, Unge M (2011) In *2011 IEEE Int Conf Dielectr Liq*, 1–5
- [29] Fdez Galván I, Elena Martín M, Muñoz-Losa A, Aguilar MA (2009) *J Chem Theory Comput* **5**:341–349
- [30] Åstrand PO, Ramanujam PS, Hvilsted S, Bak KL, Sauer SPA (2000) *J Am Chem Soc* **122**:3482–3487
- [31] Wong P, Forster E (1982) *IEEE Trans Electr Insul* **EI-17**:203–220
- [32] Bonifaci N, Denat A (1991) *IEEE Trans Electr Insul* **26**:610–614
- [33] Beroual A (1993) *J Appl Phys* **73**:4528–4533
- [34] Bårmann P, Kröll S, Sunesson A (1996) *J Phys D: Appl Phys* **29**:1188–1196
- [35] Ingebrigtsen S, Bonifaci N, Denat A, Lesaint O (2008) *J Phys D: Appl Phys* **41**:235204
- [36] Cool TA, Wang J, Nakajima K, Taatjes CA, McIlroy A (2005) *Int J Mass Spectrom* **247**:18–27
- [37] Jung J, Gress H (2003) *Chem Phys Lett* **377**:495–500
- [38] Carroll BW, Ostlie DA (2007) *An introduction to modern astrophysics*. Pearson Education, San Francisco, second edn.
- [39] Gournay P, Lesaint O (1994) *J Phys D: Appl Phys* **27**:2117–2127
- [40] Eschner MS, Zimmermann R (2011) *Appl Spectrosc* **65**:806–816
- [41] Naidis GV (2018) *Plasma Res Express* **1**:017001
- [42] Brownrigg JT, Kenny JE (2009) *J Phys Chem A* **113**:1049–1059
- [43] Linhjell D, Ingebrigtsen S, Lundgaard L, Unge M (2013) In *Proc Nord Insul Symp*, 191–196
- [44] Naidis GV (2015) *IEEE Trans Dielectr Electr Insul* **22**:2428–2432